Evidence-based sensor tasking for space domain awareness

Andris D. Jaunzemis

Graduate Research Assistant, Aerospace Engineering, Georgia Institute of Technology

Marcus J. Holzinger

Assistant Professor, Aerospace Engineering, Georgia Institute of Technology

Moriba K. Jah

Director, Space Object Behavioral Sciences, University of Arizona

Abstract

Space Domain Awareness (SDA) is the actionable knowledge required to predict, avoid, deter, operate through, recover from, and/or attribute cause to the loss and/or degradation of space capabilities and services. A main purpose for SDA is to provide decision-making processes with a quantifiable and timely body of evidence of behavior(s) attributable to specific space threats and/or hazards. To fulfill the promise of SDA, it is necessary for decision makers and analysts to pose specific hypotheses that may be supported or refuted by evidence, some of which may only be collected using sensor networks. While Bayesian inference may support some of these decision making needs, it does not adequately capture ambiguity in supporting evidence; i.e., it struggles to rigorously quantify 'known unknowns' for decision makers. Over the past 40 years, evidential reasoning approaches such as Dempster Shafer theory have been developed to address problems with ambiguous bodies of evidence. This paper applies mathematical theories of evidence using Dempster Shafer expert systems to address the following critical issues: 1) How decision makers can pose critical decision criteria as rigorous, testable hypotheses, 2) How to interrogate these hypotheses to reduce ambiguity, and 3) How to task a network of sensors to gather evidence for multiple competing hypotheses. This theory is tested using a simulated sensor tasking scenario balancing search versus track responsibilities.

1 Introduction

Space situational awareness (SSA) is concerned with accurately representing the state knowledge of objects in the space environment to provide better prediction capabilities for threats such as potential conjunction events. More recently, the discourse on SSA has turned toward space domain awareness (SDA), reflecting the ever-growing reality of world-wide space capabilities and the impact that decisions in the space environment can have on a global relational scale. In particular, SDA focuses on gathering actionable data to supply to decision-makers in their evaluation of hypotheses [1]. The space community as a whole suffers from a problem of producing high quantities data (in the form of tracks) but being unable to produce significant data on any specific object or event to increase understanding of that event. Currently, there are over 20,000 trackable objects in the space object catalog [2]. Due to observational constraints imposed by orbital mechanics, the limited number of space-observing sensors are unable to observe each object. This hinders the ability to reliably provide information on maneuvers or other events in space. Therefore, more emphasis is being placed on algorithms and processes that have an ability to ingest disparate data from many sources and fuse an understanding of the greater situation of the space domain.

In typical Bayesian reasoning, deterministic probabilities are placed on event hypotheses under the assumption that the only possible realizations of this hypothesis are true or false. However, in complex decision-making contexts, information is not always best-represented in this strictly binary manner, since some evidence for a particular hypothesis might also involve ambiguity. An expert might be able to confirm or refute a given set of hypotheses, but it cannot attribute belief to any hypotheses for which it is not an expert. For this reason, evidential reasoning methods, such as Dempster-Shafer theory, quantify this ambiguity in situation knowledge, leading to more realistic modeling of human analyst processes [3, 4].

The human-analyst-like approach to belief structures in Dempster-Shafer theory and the decision-making focus of SDA make the pair a promising combination. SDA focuses on actionable knowledge required for operation in the space environment without loss or degredation of capabilities and services [1]. Decision-making in SDA ranges from collecting raw observables, to identifying space object properties such as orbit state, to inferring mission types and evaluating specific threats [1]. Given this "big-data" problem, decision-makers must form hypotheses about the environment and its constituent objects, and apply available data to evaluate these hypotheses. Current techniques focus largely on collecting observables, identification of physical states and parameters, and determining functional characteristics [1]. For instance, some tasking techniques simply aim to maximize the number of collections in a given time horizon, whereas others might focus on minimizing covariance in the state estimates [5] Recent improvements in these data collection techniques include the use of Finite Set Statistics in detection and tracking [6, 7] and the classification approaches using ontologies and taxonomies [8]. Evidential reasoning has an ability to augment the previous techniques by ingesting a wide range of SDA data (e.g. observational data, correlated tracks, classification results) as evidence that is used to directly interrogate hypotheses of interest to the decision-maker.

This paper begins by introducing relevant elements of evidence-based reasoning. A binary-hypothesis approach to individual hypothesis formulation is discussed to allow decision-makers to form rigorous, testable hypotheses. A mathematical framework for decision-making in SDA sensor tasking is developed to allow interrogation of these hypotheses on the basis of removing ambiguity from the system. The application of this framework in a multi-objective framework is further developed since the subsets of the SDA problem are inherently multi-objective. Due to the combinatorial nature of these problems, a toy example relevant to SDA is developed to demonstrate applicability of this method in a reduced space.

2 Theory

In this section begin by summarizing relevant aspects of Dempster-Shafer theory, introducing terminology and notation that will be used throughout the paper. This is followed by a discussion on the relevance of ignorance in decision-making contexts, and further how decision-makers can decompose complex hypotheses into simple binary hypotheses to apply Dempster-Shafer effectively. Finally, we present the sensor tasking ignorance-based optimization methodology in Eqn. (11).

2.1 Dempster-Shafer Theory

Dempster-Shafer (D-S) theory deals with the assignment of belief to particular hypotheses based on available evidence. The set of hypotheses under consideration $\Theta = \{\theta_1, \theta_2, \ldots\}$ is called the frame of discernment. In D-S theory, the hypotheses that comprise the frame of discernment should be mutually exclusive and collectively exhaustive; in other words, exactly one of these hypotheses must be true at a given instant.

2.1.1 Basic Belief Assignments

Given a frame of discernment Θ, the function m, called the basic belief assignment (BBA), assigns belief values in the range 0 to 1 to a subset of hypotheses: $m : \theta \mapsto [0, 1], \theta \subseteq \Theta$. A BBA represents an expert's belief in each hypothesis based on the evidence available to that expert. BBAs are typically assumed to possess a few properties:

1) $\sum_{A \subseteq \Theta} m(A) = 1$
2) $m(\emptyset) = 0$

The first property ensures that the support attributed to the hypotheses in the frame of discernment adds up to 1. The second property enforces that belief is only attributed to hypotheses available in the frame of discernment.

The set of hypotheses that have non-zero belief mass are the focal set of the associated BBA. For ease of discussion, a number of common BBAs are typically defined based on their focal sets. A vacuous BBA is one in which all the belief mass is assigned to Θ, such that $m(\Theta) = 1$, $m(A) = 0 \, \forall \, A \subset \Theta$. A simple BBA is one in which the focal set consists of only two elements: the entire frame of discernment Θ and one other hypothesis, as in $m(A) = p$, $m(\Theta) = 1 - p$, $m(B) = 0 \, \forall \, B \in 2^{\Theta} \setminus \{A, \Theta\}$.

Using BBAs, Shafer defines the notions of belief and plausibility, which form lower and upper bounds on the probability that a proposition is provable given the available evidence. Belief and plausibility can be computed from a given BBA m using Eqs. (1) and (2), respectively:

$$\mathrm{bel}\,(A) = \sum_{B \subseteq A} m(B) \tag{1}$$

$$\mathrm{pl}\,(A) = \sum_{B \cap A \neq \emptyset} m(B) = 1 - \mathrm{bel}\,(\neg A) \tag{2}$$

where $\neg A$ is the negation, or complement, of hypothesis A. In other words, the expert's belief in, or support for, hypothesis A, is composed of the sum of the belief masses attributed to A and its subsets. The plausibility of hypothesis A is composed of the sum of the belief masses attributed to any hypothesis whose intersection with hypothesis A is non-empty. Also note that, since the truth-set Θ represents the disjunctive combination of an exhaustive set of hypotheses, the belief and plausibility of the truth-set must both be equal to 1.

2.1.2 Combination Rules

Numerous methods exist for combining BBAs from multiple experts to form a fused mass function [9]. The new mass function behaves just like any other BBA, so a fused understanding of belief and plausibility can be obtained. Each combination method exhibits slightly different properties, so implementation should take into consideration use-cases of this fused belief and characteristics of the evidence sources. A common BBA combination technique is Dempster's conjunctive rule, which is commutative, associative, and admits the vacuous BBA. Dempster's conjunctive rule of combination, shown in Eq. (3), is often represented using the $\oplus$ operator. The belief mass attributed to hypothesis $A \subseteq \Theta$ after combination of BBAs from experts i and j is given as:

$$m_{i \oplus j}(A) = (m_i \oplus m_j)(A) = \frac{\sum_{B \cap C = A} m_i(B) m_j(C)}{1 - K} \tag{3}$$

$$K = \sum_{B \cap C = \emptyset} m_i(B) m_j(C) \tag{4}$$

where K is a term that accounts for conflict between the bodies of evidence. The use of the conflict term K in Eqn. (3) has the effect of attributing conflicting evidence to the null-set. Since support cannot be attributed to the null-set (in classical Dempster-Shafer theory), this belief mass is normalized across the remaining hypotheses [9].

Some uses of Dempsters rule lead to counter-intuitive results in the presence of extreme conflict, an observation typically referred to as Zadehs paradox [10]. However, the scenario in Zadehs paradox can be resolved by more carefully adhering to Cromwells Rule, i.e. not assigning a probability of exactly 0 or 1 to any particular prior. This caveat, with the inclusion of the open-world assumption, i.e. admitting that the actual true event might lie outside the theorized set of possible events, led to the development of the Transferable Belief Model (TBM) as a derivative of Dempster-Shafer theory [11]. The constraints of this particular application allow the classical Dempster-Shafer implementation to be appropriate without applying TBM.

It is important to note that Dempsters rule is not idempotent. Subsequent evidence is assumed to be statistically independent of previous evidence. Therefore, when using Dempsters rule, the evidence must be assumed to be distinct; otherwise, repeated evidence will be heavily weighted in the fused belief mass.

Dempster's rule is also not the only combination rule for BBAs. For instance, Yager developed a related class of combination rules that, like Dempster's rule, are commutative and not idempotent, but in Yager's case the rule is quasi-associative [12, 13]. The primary difference in Yager's method is the use of a separate probability structure, the ground probability assignment, to pool evidence before conversion to a BBA [9]. Instead of normalizing out conflict, evidence from conflicting evidence is attributed to the universal-set, the frame of discernment Θ. As such, Yager's rule is also called the unnormalized Dempster's rule, and indeed in the case of no conflict both methods yeild the same result [9].

Additional combination rules have been developed that do enforce idempotence, which can be employed in the case of non-distinct bodies evidence. While the above methods are conjunctive (AND-based) in the attribution of evidence to hypothesis-intersections, alternate methods employ disjunctive (OR-based) to handle evidence from varying-reliability sources [9].

For a more complete discussion on important developments in Dempster-Shafer theory, Yager and Liu compiled a book of classic works, reviewed by Dempster and Shafer, on the theory of belief functions [14].

2.2 Importance of Ignorance

Dempster-Shafer and other evidential reasoning theories do not require an expert to report belief in only singleton hypotheses. Instead, the focal set can contain any subset of the frame of discernment, including the entire frame of discernment itself. This particular hypothesis is referred to as the universal-set, so-called because it is, by definition, the disjunctive combination of all the mutually exclusive and collectively exhaustive hypotheses. The hypothesis $A = \Theta$ is surely true; one of these hypotheses must have occurred given the exhaustive nature of the frame of discernment. However, attributing belief mass to Θ does not increase an analyst's understanding of the situation. Instead, it represents a residual ambiguity, indicating that the expert was unable to attribute that belief to any particular hypothesis. This admits an ignorance on the part of the expert that is crucial in modeling realistic decision-making environments.

Similarly, contributing belief to any non-singleton subset of hypotheses admits some ignorance (e.g. note the indeterminism in the statement "I attribute X belief to either A or B"), since the expert is saying it is unable to further delineate between those hypotheses based on its available evidence. When considering potential courses of action, the ideal course leads to a state of perfect knowledge and no residual ambiguity; in other words, all belief is attributed solely to singleton hypotheses. This idea of ignorance is essential to our approach to tasking in SDA: to support the objectives of decision-makers, their hypotheses must be possible to interrogate with evidence, with the goal of confirming or rejecting the hypotheses. This can be alternately formulated as a minimization of ignorance in the hypothesis space. In a similar way that covariance-reduction techniques aim to approach the truth of the estimated state (e.g. orbit) given the available data, a tasking scheme focused on ignorance-reduction will yield the truth-or-falseness of that hypothesis given the available evidence.

2.3 Binary Hypothesis BBAs

From Eqn. (3) It can be seen that the computational complexity of the combination of two BBAs scales quadratically with the number of hypotheses in the frame of discernment. The $\mathcal{O}(n^2)$ nature of Dempster's rule means it is computationally preferable to restrict the number of hypotheses n in Θ. The simplest and most computationally attractive frame of discernment is therefore a binary frame where the two hypotheses are simply a null and alternate hypothesis: $\Theta = \{\theta, \neg\theta\}$ where the $\neg$ symbol indicates the negation of hypothesis θ. Using first order logic, a complicated frame of discernment an be decomposed into a number of subsets of frames, each addressing smaller portions of information. The important aspect to consider is that the hypotheses being formed must be able to be interrogated through data that is currently available or actionable. The relevant action can then gather evidence to directly interrogate this hypothesis, feeding a BBA that represents that particular expert.

Utilizing a binary hypothesis structure allows the combined BBA to be written simply:

$$K_{i,j} = m_i(\theta)m_j(\neg\theta) + m_i(\neg\theta)m_j(\theta) \tag{5}$$

$$m_{i\oplus j}(\theta) = \frac{m_i(\theta)m_j(\theta) + m_i(\theta)m_j(\Theta) + m_i(\Theta)m_j(\theta)}{1 - K_{i,j}} \tag{6}$$

$$m_{i\oplus j}(\neg\theta) = \frac{m_i(\neg\theta)m_j(\neg\theta) + m_i(\neg\theta)m_j(\Theta) + m_i(\Theta)m_j(\neg\theta)}{1 - K_{i,j}} \tag{7}$$

$$m_{i\oplus j}(\Theta) = \frac{m_i(\Theta)m_j(\Theta)}{1 - K_{i,j}} \tag{8}$$

Additionally, in this case, the ignorance in frame Θ associated with BBA m is simply the belief attributed by m to the whole frame, since it is the only non-singleton hypothesis:

$$\mathrm{ig}\,(\Theta) = m(\Theta) \tag{9}$$

In the next section, we give an example of how BBAs can be constructed for some classic SDA sensors.

2.4 SDA Sensors as Dempster-Shafer Experts

In order to apply Dempster-Shafer reasoning, available SDA sensors must be cast as Dempster-Shafer experts, using that sensor's data as evidence to contribute belief mass to the available hypotheses. In this paper, we are concerned with the tasking of electro-optical (EO) sensors such as telescopes. A number of physical properties of the sensor must be provided for simulation, such as focal length and pixel size. Information on the observation environment is also available in the form of cloud cover detection, sky brightness estimation, an observatory weather station, and local weather forecasting. This particular arrangement represents the available sensors for the Georgia Tech observatory, which is home to the Georgia Tech Space Object Research Telescope (GT-SORT), a half-meter Raven-class telescope.

The radiometric model developed by Coder et al. [15] is used to compute the probability of detection of an RSO for a given EO sensor. To compute the probability of detection of an RSO for an EO sensor, the radiometric model in Eqn. (10), developed by Coder et al., is used [15]:

$$P_d\left(I_{sky}, tr_{atm}\right) = \frac{1}{2}\left[1 - \mathrm{erf}\left(\frac{SNR_{alg}\sigma_n - \mu_{so}}{\sqrt{2}\sigma_{so}}\right)\right] \tag{10}$$

where the relevant terms are: I_{sky} background sky irradiance measured in $\left(\frac{m_v}{\mathrm{arcsec}^2}\right)$, tr_{atm} atmospheric transmittance, SNR_{alg} is the required SNR for a successful detection based on the chosen detection algorithm. The remainder of the terms and their methods of calculation are discussed at length in [15]. Importantly, this model provides the ability to ingest information from the aforementioned sensors and form BBAs. Preliminary work [16] showed how sensors available at the Georgia Tech Observatory, particularly an All-Sky camera and sky brightness monitor, could be used to fuse a better understanding of the observation environment, incorporating that real-time data into the tasking algorithm through Eqn. (10). Using the probability from Eqn. 10 as belief in the hypothesis that an object will be detected, for instance, the belief and ignorance can be pooled for all sensors. This will be demonstrated in the simulated scenario below.

2.5 Ignorance-Based Optimization

In the case that a decision-maker is only concerned with a single hypothesis, the above formulation focused on minimizing ignorance can be implemented as a single-objective optimization problem. However, most interesting tasking problems occur where there are multiple competing objectives, such as the "search vs track" scenario. In this case, allocation of sensor resources to address one objective will necessarily hinder progress in another objective.

One approach to multi-objective optimization involves the minimization of the weighted-sum of the competing objectives. This approach allows the decision-maker to specify the degree to which he/she is concerned with a particular hypothesis and adjust tasking accordingly.

To formalize the optimization problem, let us define the set of all possible actions as $\mathcal{A}$ and the set of all relevant hypotheses $\mathcal{H}$. At a given epoch t_k, each action $A_{i,k:k+1}$ acts on the current understanding of the environment H_k to gather new information and update the relevant hypotheses

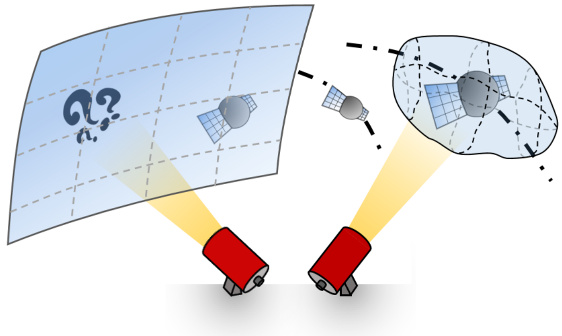

Figure 1: Search versus Track scenario illustration.

at the next time instant, $A_{i,k:k+1}(H_k) \mapsto H_{k+1}$. The total sum of ignorance in the hypotheses H_k can be calculated as $\text{ig}(H_k) = \text{ig}(H_{1,k}) + \text{ig}(H_{2,k}) + \ldots + \text{ig}(H_N, k)$. Therefore, given a set of N weightings for N hypotheses $\mathcal{W} = \{w_1, w_2, \ldots, \ldots N\}$ the set of decisions $\mathcal{D}_{k:k+M-1} \in \mathcal{A}_{k:k+1} \times \ldots \times \mathcal{A}_{k+M-1:k+M}$ taken from times $t_k, \ldots, t_{k+M}$ can be determined to minimize weighted total ignorance at the final time-step as follows:

$$\begin{aligned} \mathcal{W} &= \{w_1, w_2, \ldots, \ldots N\} \\ \mathcal{A}_{k:k+1} &= \{A_{1,k:k+1}, A_{2,k:k+1}, \ldots\} \\ \mathcal{H}_k &= \{H_{1,k}, H_{2,k}, \ldots, H_{N,k}\} \\ \mathcal{D}_{k:k+M-1} &\in \mathcal{A}_{k:k+1} \times \ldots \times \mathcal{A}_{k+M-1:k+M} \\ \min_{\mathcal{D}_{k:k+M-1}} \text{ig}(H_{k+N}) &= \sum_{i=1}^{N} w_i \text{ig}(H_{i,k+N}) \end{aligned} \tag{11}$$

Varying the weights and re-evaluating the objective function generates a list of candidate solutions to minimize weighted total ignorance. The non-dominated points, with respect to ignorance in each individual hypothesis, form a pareto frontier [17]. That is to say, any point on that surface can be considered an optimal solution to this tasking problem.

Notice that the decision set $\mathcal{D}_{k:k+M-1}$ is an element from the Cartesian product of action spaces. It is this search space to find the optimal decision set that makes this problem, like the well-known Traveling Salesman problem, NP-complete. The addition of a selection of weightings further increases the dimensionality of the problem, making long-time-horizon solutions with many different hypotheses and actions computationally intractable. Therefore, the simulations in this paper will deal with a simplified example that is computationally feasible at least in small time steps.

3 Simulation Results

A search-versus-track simulation, illustrated in Fig. 3, is presented to evaluate the validity and applicability of the theoretical results to realistic SDA scenarios. In this simulation, a single sensor is tasked with tracking two space objects, one in low-Earth-orbit (LEO) and the other in Geostationary orbit (GEO). Additionally, the sensor is tasked to search for new space objects not already in the catalog. Therefore, the decision-making process is a multi-objective optimization problem, trading between these three objectives (track object 1, track object 2, or search).

3.1 Hypothesis Formulation

The first step in applying Dempster-Shafer theory to this problem is to rigorously define hypotheses to be interrogated. In particular, we endeavor to formulate binary hypotheses to lessen the computational burden in evidence combination and computing ignorance.

3.1.1 Search

The goal of the search phase is to look for new space objects that are not in the space object catalog. The hypotheses can be stated simply as:

θ_S - An observation yields successful detection of a new space object.

$\neg\theta_S$ - An observation does not yield successful detection of a new space object.

To provide evidence for search, a prior distribution is developed using space object catalogs. This is based of the assumption that an electro-optical sensor is Specifically, the Space-Track.org catalog is used for TLE data, and the Celestrak catalog is used for auxiliary space object data, such as radar cross-section. The prior is computed by propagating the entire space object catalog for a simulated 24-hours, generating a sampling of unit-vectors in inertial space. A Gaussian kernel (with 10 m 1-sigma uncertainty) is convolved across each of the unit-vectors to form a probability density function (PDF) for the locations of space objects averaged over one day.

The PDF is further refined by accounting for observation conditions using Earth-shadow and solar phase angle. Using a simple cylindrical Earth-shadow model [18], if the object is deemed to be in Earth-shadow (both conditions met in Eqn. (12)) its probability density is zeroed out.

$$0 \leq \|\mathbf{r}_{sun} \times \mathbf{x}_{so}\| - R_E \tag{12}$$

$$0 \leq \mathbf{r}_{sun} \cdot \mathbf{r}_{so} \tag{13}$$

Similarly, solar phase angle ϕ (the angle formed by the space object and the sun from the perspective of the observer) is considered by scaling the mean of the relevant Gaussian component by $\frac{\phi}{180}$. If ϕ is near 0-degrees (space object directly between Earth and Sun), its probability density is significantly discounted. These constraints ensure that the prior PDF of space objects includes only those objects in good optical observation conditions. Finally, the PDF is transformed into local look-angle (azimuth-elevation) space for the observer at each simulation time epoch and re-normalized to include only those space objects above the horizon (elevation ≤ 0). The final PDF can be interrogated to find the region of highest space object density to provide a region to search.

A sample contour plot of the PDF can be seen in Fig. 2 in two coordinate systems: right ascension-declination and azimuth-elevation. On these contours, the dark regions represent higher densities of observable space objects. Note that the extreme declinations show the highest densities near the poles, matching intuition for dense regions of space. The GEO belt also stands out at zero declination, though portions of the GEO belt are discounted due to solar phase angle. The azimuth-elevation data is shown in a polar plot, with the center representing 90-degrees elevation (directly overhead) and azimuth increasing clockwise from north at the top.

Now the prior PDF P_s can be used to provide evidence for the search hypotheses in planning the sensor schedule. At each time step (t), the search region (az, el) with the highest space object density is selected, yielding the following binary BBA for search, m_s:

$$m_s(\theta_s) = P_s(t, az, el) \quad , \quad m_s(\neg\theta_s) = 0 \quad , \quad m_s\left(\{\theta_s, \neg\theta_s\}\right) = 1 - P_s(t, az, el) \tag{14}$$

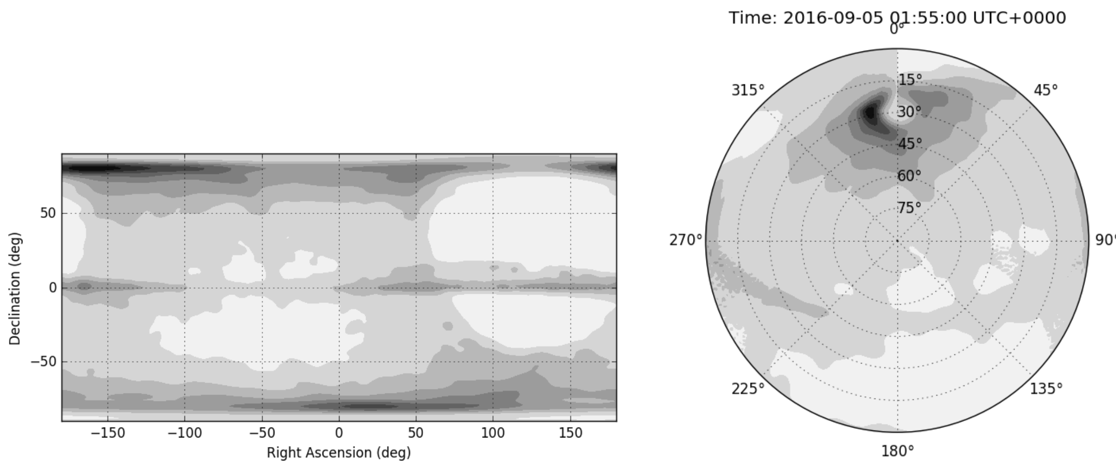

(a) Right-ascension and declination

(b) Azimuth and elevation

Figure 2: Search prior PDFs based on space object catalogs

Note that the space object density at any given search area is typically very low ($P_s(t, az, el) \leq\leq 1$), so the amount of evidence gained (or ignorance lost) through a search action is similarly low.

3.1.2 Track

The goal of the track phase is to track objects that are not in the space object catalog. The hypotheses can be stated simply as:

θ_T - An observation yields successful detection of the tracked object.

$\neg\theta_T$ - An observation does not yield successful detection of the tracked object.

The BBA for track is more complicated than that for search, since the θ_T hypothesis can be decomposed into a number of parts. In order to guarantee successful detection, the space object needs to be visible (above the horizon), detectable (in favorable observation conditions), and its position uncertainty must be contained the field of view of the sensor.

Testing for visibility is straightforward: the space object elevation must be above a threshold value based on the observing environment (e.g. 20 deg to clear the skyline in Atlanta):

$$P_v = 1 \quad \text{if } el[t] >= el_{threshold} \tag{15}$$

$$= 0 \quad \text{else} \tag{16}$$

Detectability involves more effort to account for the local observation conditions, including cloud cover and sky brightness. Equation (10) is used here again to compute the probability of detection, P_d, given the local conditions.

Finally, the uncertainty requirement enforces that the covariance remain within certain bounds. The associated probability is computed by determining the volume of the covariance ellipse that is intersected by the field of view after rotating the covariance into the observer's frame.

$$P_c = 1 \quad \text{if covariance within FOV} \tag{17}$$

$$= \frac{A_{fov}}{A_{cov}} \text{ else} \tag{18}$$

Table 1: GT-SORT Sensor Properties

Property	Value	Units
Latitude	33.7756	deg
Longitude	-84.3963	deg
Altitude	200	m
Focal Length	3.0	m
Resolution	(2736, 2192)	px
Field of View	(14.2, 11.4)	arcmic
IFOV	0.312	arcsec

Having computed the component probabilities, the binary BBA for track is computed as follows, m_t:

$$m_t(\theta_t) = P_v(t, el) * P_d(t, az, el) * P_c(t, az, el) \tag{19}$$

$$m_t(\neg\theta_t) = 0 \quad , \quad m_t(\{\theta_t, \neg\theta_t\}) = 1 - P_v(t, el) * P_d(t, az, el) * P_c(t, az, el) \tag{20}$$

This formulation has the effect of ensuring that ignorance associated with the track hypothesis is low only when the detection, visibility, and covariance are within expected values.

3.2 Optimization Problem

Following the formulation in Eqn. (11), the optimization problem relevant to this simulated scenario is defined as follows:

$$\begin{aligned}
\mathcal{W} &= \{w_1, w_2, w_3\} \\
\mathcal{A}_{k:k+1} &= \{T_{1,k:k+1}, T_{2,k:k+1}, S_{k:k+1}\} \\
\mathcal{H}_k &= \{\Theta_{T_1,k}, \Theta_{T_2,k}, \Theta_{S,k}\} \\
\mathcal{D}_{k:k+M-1} &\in \mathcal{A}_{k:k+1} \times \ldots \times \mathcal{A}_{k+M-1:k+M} \\
\min_{\mathcal{D}_{k:k+M-1}} \text{ig}\left(H_{k+M}\right) &= \sum_{i=1}^{3} w_i \text{ig}\left(H_{i,k+M}\right) \\
&= w_1 m_{T_1}(\Theta_{T_1,k+M}) + w_2 m_{T_2}(\Theta_{T_2,k+M}) + w_3 m_S(\Theta_{S,k+M})
\end{aligned} \tag{21}$$

where $w_1 + w_2 + w_3 = 1$ and M is the chosen time horizon.

3.3 Implementation Details

The simulations begin on September 4, 2016, 20:59:00 EST and end on September 4, 2016, 21:19:00 EST. The sensor cadence is set to 1 minute, meaning there are 20 tasking decision epochs. Even in this low dimensional problem, analyzing all permutations of 3 actions over 20 time steps yields well over 3-billion candidate schedules. This longer time horizon could not be computed in a reasonable amount of time, so instead a receding horizon is used. The scheduler optimizes over a smaller time range to compute the optimal schedule based on weighted total ignorance at the end of the horizon. The first step of this schedule is implemented, and then the scheduler horizon recedes a step to recompute based on the new end-of-horizon status.

Sensor properties are taken from GT-SORT, as shown in Table 1

Space-track and Celestrak catalogs were both downloaded on September 4, 2016. A GEO satellite (Echostar 11) and LEO satellite (Envisat) were selected as the tracked objects. Each TLE is propagated using SGP4 through the simulation time range to compute the observation geometries. Covariances are propagated using an Extended Kalman Filter (EKF), with measurements gathered in right-ascension declination space and measurement noise equal to the instantaneous field of view (IFOV) of GT-SORT.

For the search hypothesis, the space object density prior is created using the downloaded catalogs and averaged over September 4, 2016.

For simplicity of this report, equal weighting is applied across all three hypotheses.

3.4 Scenario: Clear Dark Sky

In this set of results, the sky brightness and cloud cover are both non-factors; the optical probability of detection is 1 throughout the simulation. The horizon- and covariance-based estimations are still a factor, though, and affect the projected ignorance-loss due to the track actions.

3.4.1 Greedy Optimization

The greedy optimization results in Fig. 4(a) show both computed optimal algorithm performance and a snapshot of the simulation in progress. The polar plots show azimuth (around circumference, North at top) and elevation (radially outward, directly up at center) with the space object density data superimposed over spacecraft tracks. Blue triangles indicate current position, and the red square indicates the sensor's current action. The time-series data shows the schedule taken at top and the ignorance in each hypothesis at each time step.

These results demonstrate an ability to reduce ignorance quickly. The GEO and Search areas are both detectable to start, but the ignorance reduction in the GEO observation is significantly greater at step one, so it is chosen as the action. Further ignorance cannot be reduced in the GEO observation, so the sensor switches to Search until the LEO object enters and satisfies the minimum elevation requirement. As the LEO object's uncertainty evolves during propagation, its ignorance begins to rise again as the covariance exceeds the field of view. Therefore, it is observed again, this time reducing a slightly different portion of the covariance due to the change in observation geometry. Without a prediction horizon, however, this scheme oscillates between the remaining viable options for ignorance reduction (Search and Track LEO).

3.4.2 5-step Horizon

In Figs. 4(b) and 4(c), we see the same initial schedule, ignorance, and spatial data from the greedy tasking simulations. In the 5-step horizon case, the sensor performs similar to the greedy approach until the LEO tracking phase. This time, it recognizes that it can minimize the LEO covariance (and thereby the ignorance) at the end of the simulation by observing it at the last possible time step. This allows the sensor to continue to search for new objects and avoids the task mode oscillation seen in the greedy approach.

3.5 Scenario: Dark Sky with Clouds

The final simulated data concerns a but dark night with clouds. Cloud cover is simulated in the northern portion of the sky, where the LEO space object exits the field of view. The cloud-covered greedy simulation results have been omitted from this section since they are similar to the greedy results in clear skies.

3.5.1 5-step Horizon

Figure 4 shows the resulting cloudy night simulations. In good observation conditions, the algorithm would want to get one more detection before the LEO object exits to minimize ignorance from the covariance expanding. However, here the sensor pivots to look for the LEO object earlier,

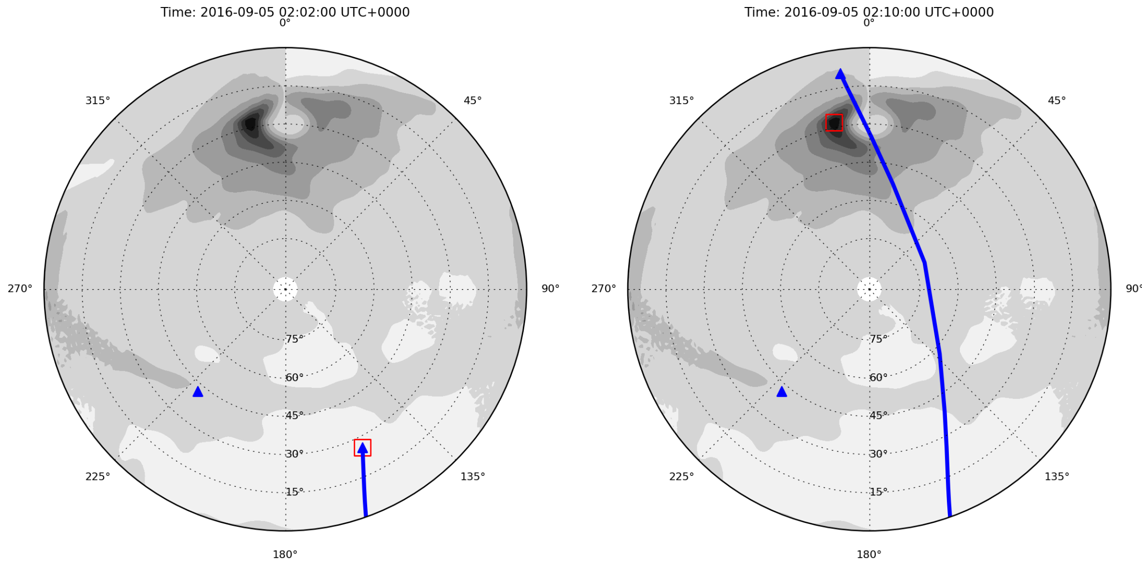

(a) Clear, greedy approach (Track LEO)

(b) Clear, 5-step horizon (Search)

Figure 3: GT-SORT

just before it enters the cloudy skies. The remainder of the simulation is similar to the previous 5-step horizon, checking GEO right away and remaining on the Search hypothesis the rest of the time.

4 Conclusions

This work applied Dempster-Shafer theory, with its ability to represent ambiguity to support decision making, to SDA, with its emphasis on actionable information. Using first-order logic to decompose complicated hypothesis spaces into binary hypotheses, the decision-maker can create a computationally-tractable set of hypotheses to investigate. The optimization approach centers around the minimization of ignorance in multiple competing objectives, providing a method of tasking that goes beyond gathering data and attempts to directly interrogate hypotheses through sensor action. Simulated results of a seach-versus-track scenario show the algorithm is able to successfully assign the sensor to track a set of objects based on the observation conditions, while also allocating resources to search for new objects.

Future work seeks to build upon this theory by applying multi-objective optimization techniques for quickly identifying non-dominated solutions in this vast decision space. The current paper used brute force to analyze all potential options, but ideally the current location on the pareto surface and its sensitivities to different decisions should lead the decision-maker to be able to optimize the weighting schedule and gather much needed actionable data.

Acknowledgements

This material is based upon work supported by the National Science Foundation Graduate Research Fellowship under Grant No. DGE-1148903.

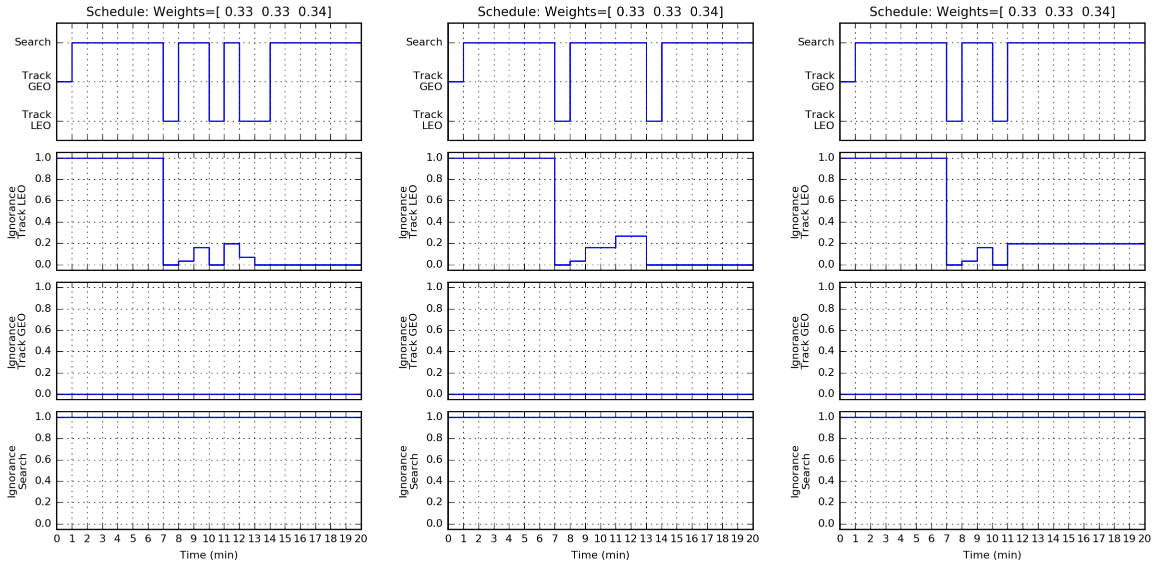

(a) Clear, greedy approach (b) Clear, 5-step horizon (c) Cloudy, 5-step horizon

Figure 4: Scheduling and ignorance results for all simulated scenarios.

References

[1] Moriba K. Jah. Space surveillance, tracking, and information fusion for space domain awareness. Technical report, 2016.

[2] J.-C. Liou. Modeling the large and small orbital debris populations for environment remediation. Technical report, NASA Orbital Debris Program Office, Johnson Space Center, Houston, TX, June 2014.

[3] Glenn Shafer. *A Mathematical Theory of Evidence*. Princeton University Press, 1976.

[4] A. P. Dempster. The dempster-shafer calculus for statisticians. *International Journal of Approximate Reasoning*, 2007.

[5] Kerric Hill, Kyle T. Alfriend, and Chris Sabol. Covariance-based uncorrelated track association. In *AIAA/AAS Astrodynamics Specialist Conference and Exhibit*, 2008.

[6] Kyle J. DeMars, Islam I. Hussein, Carolin Frueh, Moriba K. Jah, and R. Scott Erwin. Multiple-object space surveillance tracking using finite-set statistics. *Journal of Guidance, Control, and Dynamics*, pages 1–16, March 2015.

[7] I. I. Hussein, K. J. DeMars, C. Fruh, M. K. Jah, and R. S. Erwin. An aegis fisst algorithm for multiple object tracking in space situational awareness. In *AIAA/AAS Astrodynamics Specialist Conference, Guidance, Navigation and Control and Co-located Conferences*, 2012.

[8] C. Fruh, M. Jah, E. Valdez, P. Kervin, and T. Kelecy. Taxonomy and classification scheme for artificial space objects. In *AMOSTech 2013*, 2013.

[9] Kari Sentz and Scott Ferson. Combination of evidence in dempster-shafer theory. Technical report, Systems Science and Industrial Engineering Department, Thomas J. Watson School of Engineering and Applied Science, 2002.

[10] Lotif A. Zadeh. A simple view of the dempster-shafer theory of evidence and its implication for the rule of combination. *AI Magazine*, 7(2):85–90, 1986.

[11] Philippe Smets and Robert Kennes. The transferable belief model. *Artificial Intelligence*, 66(2):191–234, 1994.

[12] Ronald R. Yager. Arithmetic and other operations on dempster-shafer structures. *International Journal of Man-Machine Studies*, 25(4):357–366, 1986.

[13] Ronald R. Yager. On the dempster-shafer framework and new combination rules. *Information Sciences*, 41(2):93–137, 1987.

[14] Ronald R. Yager and Liping Liu. *Classic Works of the Dempster-Shafer Theory of Belief Functions*. Springer, 2008.

[15] Ryan D Coder and Marcus J Holzinger. Multi-objective design of optical systems for space situational awareness. *Acta Astronautica*, 2016.

[16] Andris D. Jaunzemis and Marcus J. Holzinger. Evidential reasoning applied to single-object loss-of-custody scenarios for telescope tasking. In *26th AAS/AIAA Spaceflight Mechanics Conference*, February 2016.

[17] Garret N. Vanderplaats. *Multidiscipline Design Optimization*. Garret N. Vanderplaats, 2007.

[18] Adam C. Snow, III Johnny L. Worthy, Angela den Boer, Luke J. Alexander, Marcus J. Holzinger, and David Spencer. Optimization of cubesat constellations for uncued electrooptical space object detection and tracking. *Journal of Spacecraft and Rockets*, 53(3):410–419, 2016.